EXTRACTING TASK-RELATED COMPONENTS IN FUNCTIONAL MRI

Jagath C. Rajapakse, Wei Lu

School of Computer Engineering
Nanyang Technological University, Singapore
email: {asjagath,p141035107}@ntu.edu.sg

ABSTRACT

To extract consistently and transiently task-related component maps, a novel ICA paradigm, the ICA with reference (ICA-R), is proposed. ICA-R produces only component maps corresponding to the input stimuli which are used as reference signals in the learning paradigm, and all activations corresponding to a particular stimulus are located in a single component map. Computational and memory requirements of ICA-R are much less than those required by spatial ICA or temporal ICA.

Keywords: Independent component analysis, functional MRI, ICA with reference, constrained ICA, statistical parametric mapping

1. INTRODUCTION

One of the important step in functional Magnetic Resonance Imaging (fMRI) data analysis is to determine the activation map indicating the activities of brain voxels during a task. This is usually done by statistically comparing time-series corresponding to each brain voxels with the input stimulus and generating statistical maps. The simplest of this approach is the correlation analysis [1]. In order to correct for multiple comparisons and spatial correlations, the statistical maps are further analyzed using the Gaussian random field (GRF) theory, which approach is referred to as *statistical parametric mapping* (SPM) [2]. FMRI data are corrupted by physiological noise such as heart beat, respiration, blood flow, and electronic noise of the scanners and are confounded by baseline magnetization variation of the scanner and subject's head motion [3]. Therefore, prior to the application of SPM or a simple correlation analysis, fMRI data is required to be preprocessed using filtering and corrected for artifacts. These preprocessing techniques are still mostly ad hoc and alter the original data. Another drawback of this technique is that the spatial analysis of the data is done after the analysis in the temporal-domain; a spatio-temporal analysis of functional MRI data, where spatial and temporal domain analysis is done simultaneously, is often desired [4].

Independent Component Analysis (ICA) separates underlying signals, that are mutually independent in complete statistical sense, from their linear mixtures [5]. Recently, there has been a growing interest in applying ICA to analyze fMRI data [6, 7, 8, 9, 10] in two different ways: spatial ICA (SICA) or temporal ICA (TICA). The data is decomposed into a set of spatially independent components in SICA whereas the TICA decomposes the fMRI data into a set of temporally independent components. The premise of the application of ICA to fMRI analysis is that the non-task related components in fMRI data is either independent in spatial-domain (SICA) or independent in time-domain (TICA). ICA is becoming increasingly popular for the analysis of fMRI because it can separate the component of interest, that is due to task-related brain activation, from other components that are due to interferences and artifacts. It is, therefore, unnecessary to use preprocessing of fMRI data before analyzing them for detection of brain activation. Furthermore, analysis of fMRI using ICA is spatio-temporal.

In SICA, the multifocal brain areas activated by performance of a sensory or cognitive task is presumed to be unrelated to the signal areas that are affected by the artifacts and confounds. The signals due to heartbeat, respiration and blood flow can be considered as mutually independent in time-domain because they have frequencies that are different from the task. However, the spatial independence of the effect of these signals in the brain is questionable because their influence is common to most regions of the brain. The baseline magnetization variation is also independent of the task activation (may depend on the frequency of runs if the experiment is done in different runs), and affects the whole brain. Furthermore, the motion artifacts, which may be transiently task-related, appear in the whole brain indiscriminately. Some of the sources are deterministic in nature and the component maps provided may not be unrelated spatially but may be independent in time because of their characteristics in time-domain. Therefore, it is more appropriate to assume that these noise and interference sources involved in fMRI data are independent in time-domain rather than in the spatial-domain. However, to date, SICA has dominated most applications mainly because the computational requirements of TICA has been much higher than those of SICA.

The spatial independent criteria in SICA method biased towards finding a relatively sparse and discrete component areas, and the task-related component might split into several ICA components with smaller active areas with closely related time-courses [6]. If two component processes contributed due to input activation appear in well-overlapped brain area, ICA may split the resulting activation areas into many component maps. Also, if a number of independent brain processes are active during the task, the task-related activation maps may split into different component maps. Therefore, the independent assumption may not provide a unique decomposition of the data and may not be the desired representation of the fMRI data for all processes. Nevertheless, ICA may be useful to discern activation in an exploratory manner to determine differently activated brain regions such as transiently task-related activations due to arousal and alertness, or independent brain processes involved in a task.

In general, TICA is preferable to SICA because most non-task related signals are independent in time-domain. However, because the number of voxels in the spatial domain of the brain scans is large, TICA is prohibitive in practice. In a simple experiments like finger tapping experiment, it has been demonstrated that SICA and TICA produce similar results [8]. Recent study [9] using especially designed activated paradigms each consisting of two spatio-temporal components that were either spatially and temporally uncorrelated has shown that the components in the brain activation patterns produced may be dependent on the task paradigm. Therefore, the independent components of fMRI data, produced by SICA and TICA, may be valid depending on the task paradigm.

The aim of this paper is to present an application of a novel ICA technique, referred to as *ICA with reference* (ICA-R), producing a single activation pattern that is consistently and transiently task-related. ICA-R incorporates the input stimuli into the ICA learning algorithm to produce only the task-related activation components, reducing the computational requirements for the learning, and produces activation corresponding to a particular input stimulus in a single component map. One advantage of applying ICA-R to fMRI data over simple correlation technique or SPM technique is that it is not necessary to use any preprocessing techniques. Moreover, ICA-R is a spatio-temporal technique. Only a brief explanation of ICA-R is given here, and the details are presented elsewhere [11]. In this paper, we focus on the application of ICA-R on fMRI data.

2. DEFINITIONS

FMRI image is a spatio-temporal signal consisting of a series of brain scans taken over a time. Suppose that the spatial domain Ω of the fMR image consists of n voxels, and the time-domain Θ consists of m time points. Let us denote the time-series corresponds to the j th brain voxel by the vector $\mathbf{t}_j = (t_{j1}, t_{j2}, \ldots, t_{jm})^{\mathrm{T}}$ and the brain scan corresponds to the i th time instant by the vector $\mathbf{f}_i = (f_{i1}, f_{i2}, \ldots, f_{in})^{\mathrm{T}}$. Then the fMRI image data is given by the matrix $\mathbf{F} = \{f_{ij}\} = [\mathbf{f}_1\ \mathbf{f}_2\ \ldots \mathbf{f}_m]$, where f_{ij} denotes the image intensity corresponds to the voxel intensity corresponding to the i th scan and the j th brain voxel. Let $\mathbf{T} = [\mathbf{t}_1\ \mathbf{t}_2\ \ldots \mathbf{t}_n]$, then $\mathbf{F} = \mathbf{T}^{\mathrm{T}}$.

2.1. Spatial ICA (SICA)

Let us denote the set of independent component maps in SICA by $\mathbf{c}_i$ where $i = 1, \ldots, m$. If the mixing matrix in spatial ICA is $\mathbf{M}_{\mathrm{s}}$, one can write the decomposition produced by SICA as

$$\mathbf{T} = \mathbf{M}_{\mathrm{s}}\mathbf{C}^{\mathrm{T}} \tag{1}$$

where the matrix of independent spatial components, $\mathbf{C} = [\mathbf{c}_1, \mathbf{c}_2, \ldots \mathbf{c}_m]$. SICA obtains the component maps without the knowledge of the mixing matrix or the independent sources:

$$\mathbf{C}^{\mathrm{T}} = \mathbf{W}_{\mathrm{s}}\mathbf{F}^{\mathrm{T}} \tag{2}$$

where $\mathbf{W}_{\mathrm{s}}$ denotes the demixing matrix, and ideally, $\mathbf{W}_{\mathrm{s}} = \mathbf{M}_{\mathrm{s}}^{-1}$. If the mixing matrix $\mathbf{M}_{\mathrm{s}} = [\mathbf{m}_1^{\mathrm{s}}, \mathbf{m}_2^{\mathrm{s}}, \ldots \mathbf{m}_m^{\mathrm{s}}]$, Eq. (1) can be expanded as

$$\mathbf{F}^{\mathrm{T}} = \sum_{i=1}^{m} \mathbf{m}_i^{\mathrm{s}}\mathbf{c}_i^{\mathrm{T}} \tag{3}$$

That is, the columns of the mixing matrix $\mathbf{M}_{\mathrm{s}}$ can be considered as time-series that are modulated with the corresponding component maps to produce the functional image.

2.2. Temporal ICA (TICA)

Let us denote the set of independent temporal sources in TICA by $\mathbf{s}_j$ where $j = 1, \ldots, n$. If the mixing matrix in TICA is $\mathbf{M}_{\mathrm{t}}$, one can write the decomposition produced by TICA as

$$\mathbf{F} = \mathbf{M}_{\mathrm{t}}\mathbf{S}^{\mathrm{T}} \tag{4}$$

where the matrix of the independent sources, $\mathbf{S} = [\mathbf{s}_1, \mathbf{s}_2, \ldots \mathbf{s}_n]$. TICA obtains the independent sources without the knowledge of the mixing matrix or the sources:

$$\mathbf{S}^{\mathrm{T}} = \mathbf{W}_{\mathrm{t}}\mathbf{T}^{\mathrm{T}} \tag{5}$$

where $\mathbf{W}_{\mathrm{t}}$ denotes the demixing matrix, and ideally, $\mathbf{W}_{\mathrm{t}} = \mathbf{M}_{\mathrm{t}}^{-1}$. If the mixing matrix $\mathbf{M}_{\mathrm{t}} = [\mathbf{m}_1^{\mathrm{t}}, \mathbf{m}_2^{\mathrm{t}}, \ldots \mathbf{m}_m^{\mathrm{t}}]$, Eq. (4) can be expanded as

$$\mathbf{T}^{\mathrm{T}} = \sum_{j=1}^{n} \mathbf{m}_j^{\mathrm{t}}\mathbf{s}_j^{\mathrm{T}} \tag{6}$$

That is, the columns of the mixing matrix $\mathbf{M}_{\mathrm{t}}$ can be considered as component maps that are modulated with the corresponding independent sources to produce the functional image.

3. ICA WITH REFERENCE (ICA-R)

This section describes a variation to the classical ICA paradigm, *ICA with reference* (ICA-R). A detailed analysis of ICA-R and its convergence are presented elsewhere [11].

Let us denote the time varying observed signal at time t as $\mathbf{x}(t) = (x_1(t)\, x_2(t) \cdots x_n(t))^{\mathrm{T}}$ and the blind source signal consisting of ICs as $\mathbf{c}(t) = (c_1(t)\, c_2(t) \cdots c_n(t))^{\mathrm{T}}$. The linear ICA assumes that the signal $\mathbf{x}(t)$ is a linear mixture of ICs: $\mathbf{x}(t) = \mathbf{M}\mathbf{c}(t)$, where the $n \times n$ matrix $\mathbf{M}$ represents linear memoryless mixing channels. In the present approach, we expect to demix the observed signal by a demixing matrix $\mathbf{W} = [\mathbf{w}_1\, \mathbf{w}_2 \cdots \mathbf{w}_l]^{\mathrm{T}}$ to be learned and produce outputs $\mathbf{y}(t) = (y_1(t)\, y_2(t) \cdots y_l(t))^{\mathrm{T}}$ that extract $l(< n)$ number of desired sources from the entire set of ICs $\mathbf{c}$. A set of corresponding reference signals $\mathbf{r}(t) = (r_1(t)\, r_2(t) \cdots r_l(t))^{\mathrm{T}}$ is available, that carries some information about the desired sources $\mathbf{c}$ but not identical to the corresponding desired signals. The goal here is to derive a neural network learning algorithm that satisfies the following two conditions simultaneously: (1) every individual estimated output is one of the ICs mixed in the input signal but different from other outputs, (2) each extracted IC is the closest one to the corresponding reference signal in some distance measure.

The negentropy $J(y_i)$ defines a natural information-theoretic contrast function to produce independent components [5]:

$$J(y_i) = H(y_{\mathrm{Gaus}}) - H(y_i) \tag{7}$$

where y_{Gaus} is a Gaussian random variable with the same variance as the output signal y_i, and $H(\cdot)$ is the differential entropy. Negentropy is always non-negative, and is zero when y_i has a Gaussian distribution [5]. The IC that corresponds to the maximum negentropy can be separated by optimizing $J(y_i)$ [5, 12]. A reliable and flexible approximation of the negentropy is given as [13]

$$J(y_i) \approx \rho[E\{G(y_i)\} - E\{G(\nu)\}]^2 \tag{8}$$

where ρ is a positive constant, $G(\cdot)$ can be any non-quadratic function, ν is a Gaussian variable having zero mean and unit variance. For multiple outputs, the contrast function is given by

$$\mathcal{C}(\mathbf{W}) = \sum_{i=1}^{l} J(y_i). \tag{9}$$

The closeness between each estimated output y_i and the reference r_i is measured by some norm $\varepsilon(y_i, r_i)$ which has a minimal value when y_i corresponds to the desired source. A threshold ξ_i can be used to distinguish this desired source, c^*, from other ICs such that the formula, $g_i(\mathbf{w}_i) = \varepsilon(y_i, r_i) - \xi_i \leq 0$, is satisfied only when $y_i = c^*$ among all ICs [11]. Treating $g_i(\mathbf{w}_i)$ $(\forall i = 1 \cdots l)$ as feasible constraints to the contrast function in Eq. (9), the problem of ICA-R can be modeled in the framework of constrained independent component analysis (cICA) [14]:

$$\begin{array}{ll} \text{Maximize} & \mathcal{C}(\mathbf{W}) = \sum_{i=1}^{l} J(y_i) \\ \text{Subject to} & \mathbf{g}(\mathbf{W}) \leq \mathbf{0},\ \ \mathbf{h}(\mathbf{W}) = 0 \end{array} \tag{10}$$

where $\mathbf{g}(\mathbf{W}) = (g_1(\mathbf{w}_1) \cdots g_l(\mathbf{w}_l))^{\mathrm{T}}$, and $\mathbf{h}(\mathbf{W}) = (h_1(\mathbf{w}_1) \cdots h_l(\mathbf{w}_l))^{\mathrm{T}}$ containing $h_i(\mathbf{w}_i) = E\{y_i^2\} - 1$ for $\forall i = 1 \cdots l$. The equality constraint $h_i(\mathbf{w}_i)$ has to be included to ensure that the contrast function $J(y_i)$ and the weight vector $\mathbf{w}_i$ are bounded. Using a simple transformation to convert the inequality constraint to an equality, the augmented Lagrangian function $\mathcal{L}(\mathbf{W}, \boldsymbol{\lambda}, \boldsymbol{\mu})$ corresponding to the problem in Eq. (10) is given by

$$\begin{aligned} \mathcal{L}(\mathbf{W}, \boldsymbol{\lambda}, \boldsymbol{\mu}) = & \sum_{i=1}^{l} J(y_i) - \boldsymbol{\lambda}^{\mathrm{T}}\mathbf{h}(\mathbf{W}) - \frac{1}{2}\boldsymbol{\gamma}^{\mathrm{T}} \|\mathbf{h}(\mathbf{W})\|^2 \\ & - \sum_{i=1}^{l} \frac{1}{2\gamma_i}[\max^2\{\mu_i + \gamma_i g_i(\mathbf{w}_i), 0\} - \mu_i^2] \end{aligned}$$

where $\boldsymbol{\lambda} = (\lambda_1 \cdots \lambda_l)^{\mathrm{T}}$ and $\boldsymbol{\mu} = (\mu_1 \cdots \mu_l)^{\mathrm{T}}$ are two sets of the Lagrange multipliers for equality and inequality constraints, respectively, and $\boldsymbol{\gamma} = (\gamma_1 \cdots \gamma_l)^{\mathrm{T}}$ are parameters to form the penalty terms to ensure the stable convergence of constrained optimization problem.

To find the maximum of $\mathcal{L}$, a Newton-like learning algorithm can be derived [11]:

$$\mathbf{W}_{k+1} = \mathbf{W}_k - \eta \langle \frac{1}{\boldsymbol{\delta}} \rangle \mathcal{L}'_{\mathbf{W}} \mathbf{R}_{\mathbf{xx}}^{-1} \tag{11}$$

where k denotes the iteration index, η the learning rate, $\mathbf{R}_{\mathbf{xx}}$ is the covariance matrix of the input $\mathbf{x}$, $\langle \frac{1}{\boldsymbol{\delta}} \rangle$ is a diagonal matrix with off-diagonal elements are all zeros and the diagonal is a vector $\frac{1}{\boldsymbol{\delta}} = (\frac{1}{\delta_1(\mathbf{w}_1)} \cdots \frac{1}{\delta_l(\mathbf{w}_l)})^{\mathrm{T}}$ and $\delta_i(\mathbf{w}_i) = \rho_i E\{G''_{y_i^2}(y_i)\} - \lambda_i - \mu_i E\{\varepsilon''_{y_i^2}(y_i, r_i)\}$ for $\forall i = 1 \cdots l$ obtained from the Hessian matrix $\mathcal{L}''_{\mathbf{W}^2}$, where $G''_{y_i^2}(y_i)$ and $\varepsilon''_{y_i^2}(y_i, r_i)$ are the second derivatives of $G(y_i)$ and $\varepsilon(y_i, r_i)$ with respect to y_i. The gradient of $\mathcal{L}$ is given by

$$\begin{aligned} \mathcal{L}'_{\mathbf{W}} = & \langle \boldsymbol{\rho} \rangle E\{G'_{\mathbf{y}}(\mathbf{y})\mathbf{x}^{\mathrm{T}}\} \\ & - \langle \boldsymbol{\lambda} \rangle E\{\mathbf{y}\mathbf{x}^{\mathrm{T}}\} - \langle \boldsymbol{\mu} \rangle E\{\boldsymbol{\varepsilon}'_{\mathbf{y}}(\mathbf{y}, \mathbf{r})\mathbf{x}^{\mathrm{T}}\} \end{aligned}$$

where $\langle \cdot \rangle$ represents a diagonal matrix where the diagonal is given by the vector inside; $G'_{\mathbf{y}}(\mathbf{y})$ and $\boldsymbol{\varepsilon}'_{\mathbf{y}}(\mathbf{y}, \mathbf{r})$ are the first derivatives of $G(\mathbf{y})$, and $\boldsymbol{\varepsilon}(\mathbf{y}, \mathbf{r}) = ((\varepsilon_1(y_1, r_1), \varepsilon_2(y_2, r_2), \ldots, \varepsilon_l(y_l, r_l))^{\mathrm{T}}$ with respect to $\mathbf{y}$, respectively. The learning of Lagrange multipliers $\boldsymbol{\lambda}$ and $\boldsymbol{\mu}$ is based on the gradient-ascent method:

$$\boldsymbol{\lambda}_{k+1} = \boldsymbol{\lambda}_k + \langle \boldsymbol{\gamma} \rangle \mathbf{h}(\mathbf{W}), \tag{12}$$

$$\boldsymbol{\mu}_{k+1} = \max\{\mathbf{0}, \boldsymbol{\mu}_k + \langle \boldsymbol{\gamma} \rangle \mathbf{g}(\mathbf{W})\}. \tag{13}$$

Although the constraints in Eq. (10) restrict one neuron to produce one particular IC different from the outputs of the other neurons, improper values of ξ_i in practice may cause different neurons converge to the same independent source. Instead of adjusting the threshold, which is impossible with little knowledge we have about the sources, it may be desirable to postprocess (that is, to decorrelate) the weight vectors in each learning iteration to prevent different neurons having the same independent source [15]:

$$\mathbf{W} = [\mathbf{W}\mathbf{R}_{\mathbf{xx}}\mathbf{W}^{\mathrm{T}}]^{-\frac{1}{2}}\mathbf{W} \tag{14}$$

where the inverse square root $[\mathbf{W}\mathbf{R}_{\mathbf{xx}}\mathbf{W}^{\mathrm{T}}]^{-\frac{1}{2}}$ is obtained from the eigenvalue decomposition of $\mathbf{W}\mathbf{R}_{\mathbf{xx}}\mathbf{W}^{\mathrm{T}} = \mathbf{U}\mathbf{D}\mathbf{U}^{\mathrm{T}}$ as $[\mathbf{W}\mathbf{R}_{\mathbf{xx}}\mathbf{W}^{\mathrm{T}}]^{-\frac{1}{2}} = \mathbf{U}\mathbf{D}^{-\frac{1}{2}}\mathbf{U}$ with the simple calculation of $\mathbf{D}^{-\frac{1}{2}}$ for the diagonal matrix $\mathbf{D}$.

The network is able to achieve the local convergence at the optimum point defined by the Kuhn-Tucker (KT) triple $(\mathbf{W}^*, \boldsymbol{\lambda}^*, \boldsymbol{\mu}^*)$. With a suitable closeness measure chosen and the threshold ξ_i properly selected, the system can converge to a global maximum when the Hessian matrix $\mathcal{L}''_{(\mathbf{w}_i^*)^2}$ is negative definite at the maximum [11].

4. ICA-R EXTRACTING TASK-RELATED COMPONENTS IN FMRI

This section describes how ICA-R can be used to analyze fMRI data, which is depicted in Fig. 1. The demixing matrix $\mathbf{W}$ is obtained by using the learning equations Eq. (11)-(13) of ICA-R to produce l number of the desired outputs. If i th output is $\mathbf{y}_i = (y_{i1}, y_{i2}, \ldots y_{im})^{\mathrm{T}}$, the output signal can be written as the matrix $\mathbf{Y} = [\mathbf{y}_1\ \mathbf{y}_2 \cdots \mathbf{y}_l]^{\mathrm{T}}$ which is given by

$$\mathbf{Y} = \mathbf{W}\mathbf{F} \tag{15}$$

The temporal independence of time courses of the functional MR data is presumed here. The input stimulation, which is known to the experimenter, is used as the reference. If i th reference is $\mathbf{r}_i = (r_{i1}\, r_{i2} \cdots r_{im})^{\mathrm{T}}$ where r_{ij} denotes j th time sample of the i th reference signal, the set of reference signals is given by the matrix $\mathbf{R} = [\mathbf{r}_1\, \mathbf{r}_2\, \cdots \mathbf{r}_i\, \cdots \mathbf{r}_l]^{\mathrm{T}}$,

The closeness between an output and the corresponding reference is defined as the negative of the correlation: $\varepsilon_i(\mathbf{y}_i, \mathbf{r}_i) = -E\{y_{ij}\, r_{ij}\}$ for $\forall j \in \Theta$. This distance is minimum when the output is maximally correlated with the reference. For comparison, the output signal $\mathbf{y}_i$ and the reference signal $\mathbf{r}_i$ are normalized to have unit variances. Then, the approximate Newton learning rule in Eq. (11) for updating the weight matrix $\mathbf{W}$, becomes:

$$\mathbf{W}_{k+1} = \mathbf{W}_k - \eta\langle\frac{1}{\boldsymbol{\delta}}\rangle\mathcal{L}'_{\mathbf{W}_k}(\mathbf{F}\mathbf{F}^{\mathrm{T}})^{-1} \tag{16}$$

where the gradient $\mathcal{L}'_{\mathbf{W}}$ is given by

$$\mathcal{L}'_{\mathbf{W}} = \langle\boldsymbol{\rho}\rangle G'(\mathbf{Y})\mathbf{F}^{\mathrm{T}} - \langle\boldsymbol{\lambda}\rangle\mathbf{Y}\mathbf{F}^{\mathrm{T}} + \frac{1}{2}\langle\boldsymbol{\mu}\rangle\mathbf{R}\mathbf{F}^{\mathrm{T}}$$

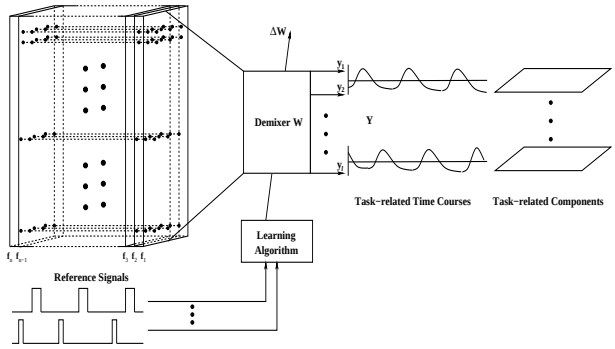

Fig. 1. Illustration of the extraction of the task-related fMRI time responses from the fMRI image, using ICA-R with the input stimulations as references.

and $\delta_i(\mathbf{w}_i) = \bar{\rho}_i E\{G''_{y_i^2}(y_i)\} - \lambda_i$ for $\forall i = 1, \cdots, l$. In an fMRI experiment, since the number of image scans, m, is usually smaller than the number of brain voxels, n, the learning rule can be further simplified as

$$\mathbf{W}_{k+1} = \mathbf{W}_k - \eta\langle\frac{1}{\boldsymbol{\delta}}\rangle\left[\langle\boldsymbol{\rho}\rangle G'(\mathbf{Y}) - \langle\boldsymbol{\lambda}\rangle\mathbf{Y} + \frac{1}{2}\langle\boldsymbol{\mu}\rangle\mathbf{R}\right][\mathbf{F}^{\mathrm{T}}]^{+} \tag{17}$$

where $[\,\cdot\,]^{+}$ denotes the pseudo-inverse of a non-square matrix. Incorporating the learning rules for Lagrange multipliers $\boldsymbol{\lambda}$ and $\boldsymbol{\mu}$ in Eqs. (12) and (13), we obtain the learning algorithm to extract only task-related time responses, using ICA, with the input stimuli as the references. The weight matrix may be also postprocessed by the decorrelation of Eq. (14) to prevent different outputs converged into the same time response.

Because the stimulation time courses usually have sub-Gaussian distributions, the practical functions used for $G(\cdot)$ should be a function growing faster than quadratic [16]. We use $G(y) = y^4/4$ to ensure the convergence of our algorithm as the Hessian matrix is always negative definite for such functions [11]. All the output time courses are statistically independent when the algorithm is converged. The corresponding activation map $\mathbf{c}^*$ can be obtained by multiplying the functional brain images $\mathbf{F}$ with the task-related time response $\mathbf{y}^*$: $\mathbf{c}^* = \mathbf{F}\mathbf{y}^*$

5. EXPERIMENTS

The experiments, namely the visual task and memory retrieval task were performed at 3.0 Tesla Medspec 30/100 scanner at the MRI Center of the Max-Planck-Institute of Cognitive Neuroscience. The images were analyzed using SPM, SICA and ICA-R techniques. In order to find the significantly activated voxels in SPM analysis, a cluster size threshold of 3 and p-value of 0.05 was used. To find and display voxels contributing significantly to a component map, the map values were scaled to z-values; voxles whose absolute z-values greater than 2.0 were considered as the active voxels. Z-statistical scores of the detected significant

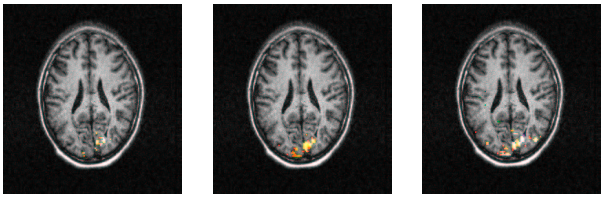

(a) (b) (c)

Fig. 2. Visual experiment: task-related activation detected by (a) SPM (b) SICA and (c) ICA-R techniques.

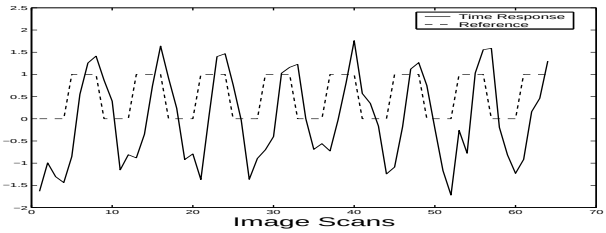

Fig. 3. Visual experiment: time course corresponding to the task-related activation detected by ICA-R.

blobs were superimposed on to the corresponding anatomical slices for visualization.

5.1. Visual Experiment

An 8KHz alternating checker board pattern with a central fixation point was projected on an LCD system, and subjects were asked to fixate on the point of stimulation. FLASH images at three axial levels of the brain at the visual cortex were taken [17]. The detected activation using the SPM, SICA and ICA-R are shown in the Fig. 2, and Fig. 3 shows the time-series corresponds to the activation pattern detected from the first axial slice using ICA-R technique.

5.2. Memory Retrieval Task

The subjects performing the experiment learned three different sets of letters (of sizes 4, 6 and 8) prior to the actual experiments with a corresponding cue for each set. During each trial, a cue for the set and a letter (probe) were presented and the subject decided whether the letter corresponded to the indicated set. Each stimulation period had two successive stimulation On-states followed by seven stimulation Off-states. The stimulations were repeated for forty eight cycles. The processes involved in the brain during the experiment include encoding of the cue and probe, retrieval of information from the secondary memory, scanning of the primary memory, response selection, and response execution [18]. The activation detected by ICA-R and SPM techniques at two axial levels of a brain of a representative subject are shown in Fig. 4. Activation detected by SPM and ICA-R were similar, but the detected activation for ICA-R were more focal to the cortical areas. The corresponding time responses detected by the ICA-R technique

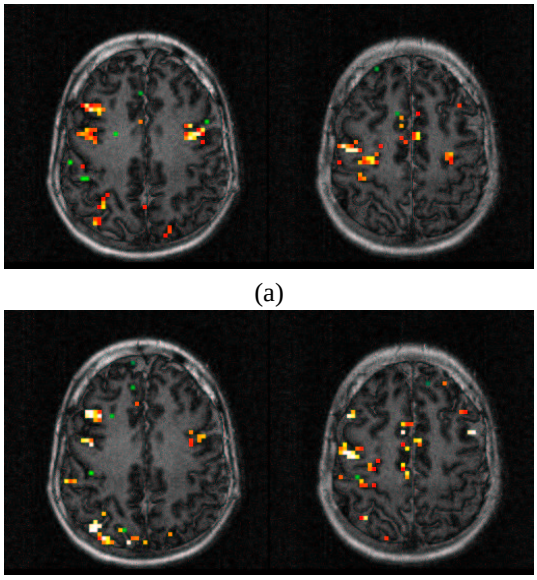

(a)

(b)

Fig. 4. Memory retrieval experiment: detected activation on two axial slices from a representative subject, obtained using (1) SPM and (2) ICA-R techniques. The white blobs represent the activations.

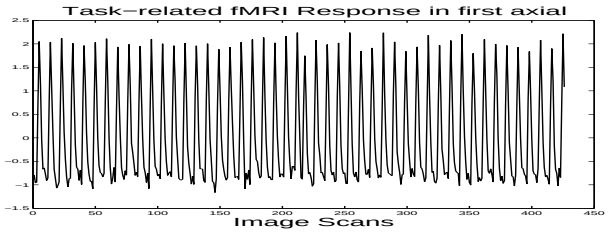

Fig. 5. FMRI time response detected from the first axial slice in the memory retrieval experiment using the ICA-R.

are shown in Fig. 5. Also the activation was detected by ICA; the activation appear in number of component maps. Two component maps corresponding to the task-related activations are shown in Fig. 6.

6. CONCLUSIONS

Application to ICA-R for analysis of fMRI data was demonstrated, which incorporates the input stimuli as the reference signals into the contrast function. ICA-R produces only the task-related component of ICA discarding all other components mutually indepdent to the task-related component. Therefore all scanner noise and interference signals are automatically removed from the resulting activation pattern. The ICA-R technique is a spatio-temporal technique unlike techniques based on correlation analysis and SPM. ICA-R technique does not split the task related component into a number of components corresponding to independent processes such as consistently task-related and tansiently task-

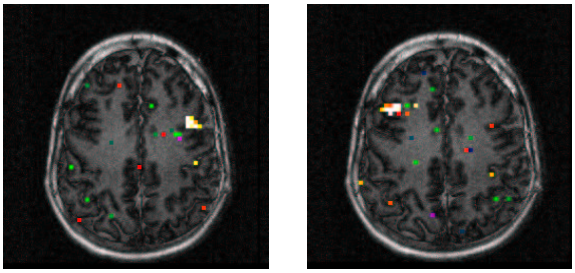

(a) (b)

Fig. 6. Two component maps of activation patterns appearing when detected by the SICA technique in memory retrieval task.

related components: all activation corresponding to a single stimulus appear in a single component unlike classical ICA. The memeory and computational requirements of ICA-R are less than those of SICA or TICA because only the task-related component maps are desired.

7. REFERENCES

[1] P. A. Bandettini, A. Jesmanowicz, E. C. Wong, and J. S. Hyde, "Processing strategies for time-course data sets in functional MRI of the human brain," *Magnetic Resonance in Medicine*, vol. 30, pp. 161–173, 1993.

[2] K. J. Friston, "Statistical parameter mapping," in *Functional Neuroimaging: Technical Foundations*, R. W. Thatcher, M. Hallett, T. Zeffiro, W. R. John, and M. Huerta, Eds. Academic Press, 1994.

[3] J. V. Hajnal, R. Myers, A. Oatridge, J. E. Schwieso, I. R. Young, and J. M. Bydder, "Artifacts due to stimulus correlated motion in functional imaging of the brain," *Magnetic Resonance in Medicine*, vol. 31, pp. 283–291, 1994.

[4] J. Piyaratna and J. C. Rajapakse, "Spatio-temporal analysis of functional images using the fixed effect model," in *Information Processing in Medical Imaging*, Kluwer-Academic, Netherlands, 2001, pp. 752–763.

[5] P. Comon, "Independent component analysis: A new concept?," *Signal Processing*, vol. 36, pp. 287–314, 1994.

[6] M. McKeown, S. Makeig, G. Brown, T-P Jung, S. Kindermann, A. Bell, and T. Sejnowski, "Analysis of fMRI data by blind separation into independent spatial components," *Human Brain Mapping*, vol. 6, pp. 160–188, 1998.

[7] M. McKeown, S. Makeig, G. Brown, T-P Jung, S. Kindermann, and T. Sejnowski, "Spatially independent activity patterns in functional magnetic resonance imaging data during the stroop color-naming task," in *Proceedings of the National Academy of Sciences USA*, Brisbane, Australia, 1998, vol. 95, pp. 803–810.

[8] B. B. Biswal and J. L. Ulmer, "Blind source separation of multiple signal sources of fMRI data using independent component analysis," *Journal of Computer Assisted Tomography*, vol. 23, pp. 265–271, 1999.

[9] V. D. Calhoun, T. Adali, G. D. Pearlson, and J. J. Pekar, "Spatial and temporal independent component analysis of functional MRI data containing a pair of task-related waveforms," *Human Brain Mapping*, vol. 13, pp. 43–53, 2001.

[10] K. S. Petersen, L. K. Hansen, and T. Kolenda, "On the independent components of functional neuroimages," *Independent Component Analysis and Blind Source Separtion (ICA2000)*, pp. 615–620, 2000.

[11] W. Lu and J. C. Rajapakse, "ICA with reference," *Submitted to ICA 2001*, 2001.

[12] M. Girolami and C. Gyfe, "Extraction of independent signal sources using a deflationary exploratory projection pursuit network with lateral inhibition," *Vision, Image and Signal Processing, IEE Proceedings*, vol. 144, no. 5, pp. 299–306, October 1997.

[13] A. Hyvärinen, "New approximations of differential entropy for independent component analysis and projection pursuit," in *Advances in Neural Information Processing Systems 10 (NIPS*97)*, 1998, pp. 273–279.

[14] W. Lu and J. C. Rajapakse, "Constrained independent component analysis," in *Advances in Neural Information Processing Systems 13 (NIPS2000)*, MIT Press, 2000, pp. 570–576.

[15] J. Karhunen, E. Oja, L. Wang, R. Vigario, and J. Joutsensalo, "A class of neural networks for independent component analysis," *IEEE Transactions on Neural Networks*, vol. 8, no. 3, pp. 487–504, 1997.

[16] W. Lu and J. C. Rajapakse, "A neural network for undercomplete independent component analysis," in *8th European Symposium on Artificial Neural Networks*, Bruges, Belgium, April 2000.

[17] J. C. Rajapakse, F. Kruggel, J. M. Maisog, and D. Y. von Cramon, "Modeling hemodynamic response for analysis of functional MRI time-series," *Human Brain Mapping*, vol. 6, pp. 283–300, 1998.

[18] J. C. Rajapakse, F. Kruggel, S. Zysset, and D. Y. von Cramon, "Neuronal and hemodynamic events from fMRI time-series," *Journal of Advanced Computational Intelligence*, vol. 2, no. 6, pp. 185–194, 1998.